Journal Pre-proof

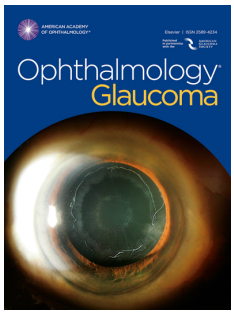

Mitochondrial Dysfunction in Primary Open-angle Glaucoma Characterized by Flavoprotein Fluorescence at the Optic Nerve Head

Davis B. Zhou, MD, Maria V. Castanos, MD, Lawrence Geyman, MD, Collin A. Rich, MSEE, PhD, Apichat Tantraworasin, MD, PhD, Robert Ritch, MD, Richard B. Rosen, MD

PII: S2589-4196(21)00285-4

DOI: https://doi.org/10.1016/j.ogla.2021.12.006

Reference: OGLA 386

To appear in: *OPHTHALMOLOGY GLAUCOMA*

Received Date: 5 June 2021

Revised Date: 18 December 2021

Accepted Date: 22 December 2021

Please cite this article as: Zhou DB, Castanos MV, Geyman L, Rich CA, Tantraworasin A, Ritch R, Rosen RB, Mitochondrial Dysfunction in Primary Open-angle Glaucoma Characterized by Flavoprotein Fluorescence at the Optic Nerve Head, *OPHTHALMOLOGY GLAUCOMA* (2022), doi: https://doi.org/10.1016/j.ogla.2021.12.006.

Title: Mitochondrial Dysfunction in Primary Open-angle Glaucoma Characterized by Flavoprotein Fluorescence at the Optic Nerve Head

Authors: Davis B. Zhou, MD*[1,2]; Maria V. Castanos, MD*[1,2]; Lawrence Geyman, MD[3,4], Collin A. Rich, MSEE, PhD[5], Apichat Tantraworasin, MD, PhD[6], Robert Ritch, MD[3]; Richard B. Rosen, MD[1,2±]
*DBZ and MVC contributed as co-first authors.

[1] Department of Ophthalmology, New York Eye and Ear Infirmary of Mount Sinai
[2] Department of Ophthalmology, Icahn School of Medicine at Mount Sinai
[3] Einhorn Clinical Research Center, New York Eye and Ear Infirmary of Mount Sinai, New York
[4] Department of Ophthalmology, Illinois Eye and Ear Infirmary, Chicago, Illinois
[5] OcuSciences Inc., Ann Arbor, MI, USA
[6] Clinical Epidemiology and Clinical Statistic Center, and Department of Surgery, Faculty of Medicine, Chiang Mai University, Chiang Mai, Thailand

[±] Corresponding Author: Richard B. Rosen, MD
New York Eye and Ear Infirmary of Mount Sinai
310 E 14th Street
New York, NY 10003
rrosen@nyee.edu

Meeting Presentation: The Association in Research in Vision and Ophthalmology Annual Meeting, 2021

Financial Support: Funding for this research was provided by the New York Eye and Ear Infirmary Research Foundation, the Marrus Family Foundation, and the Research to Prevent Blindness Foundation. The sponsor or funding organization had no role in the design or conduct of this research.

Conflicts of Interest:
Richard B. Rosen: OptoVue: Consultant & Patent; Boehringer-Ingelheim: Consultant; Astellas: Consultant; Genentech-Roche: Consultant; NanoRetina: Consultant; OD-OS: Consultant; Opticology: Personal Financial Interest; Guardion: Personal Financial Interest; Regeneron: Consultant; Bayer: Consultant; CellView: Consultant
Robert Ritch: C-MER: Consultant/Advisor; Diopsys, Inc.: Consultant/Advisor; Emerald Bioscience Inc.: Consultant/Advisor; Glauconix, Inc.: Consultant/Advisor; Guardion Health Sciences: Consultant/Advisor, Royalty; Intelon Optics: Consultant/Advisor; Ocular Instruments, Inc.: Royalty; Sanoculis: Consultant/Advisor; Sensimed: Consultant/Advisor; Xoma: Consultant/Advisor
Collin A. Rich: OcuSciences: Personal Financial Interest; Employment
Apichat Tantraworasin, Lawrence Geyman, Davis B. Zhou, Maria V. Castanos: None

Running Head: Mitochondrial Dysfunction in POAG at the Optic Nerve Head

Manuscript Word Count: 2438 / 3000

Abbreviations: optic nerve head (ONH), primary open-angle glaucoma (POAG), retinal ganglion cells (RGC), elevated intraocular pressure (IOP), normal-tension glaucoma (NTG), reactive oxygen species (ROS), flavoprotein fluorescence (FPF), circumpapillary retinal nerve fiber layer thickness (cpRNFLT), gray scale unit (gsu).

Key Words: Glaucoma, Mitochondria, Flavoprotein, Metabolic

Abstract

Objective**:** To investigate the presence of flavoprotein fluorescence (FPF) at the optic nerve head (ONH) rim as a marker of mitochondrial dysfunction in primary open-angle glaucoma (POAG) and control eyes.

Design**:** Retrospective cross-sectional study, with patients recruited from the New York Eye and Ear Infirmary of Mount Sinai.

Subjects, Participants, and/or Controls**:** A total of 86 eyes (50 eyes of 30 POAG patents and 36 eyes of 20 controls) were enrolled. The presence of POAG was defined by circumpapillary retinal nerve fiber layer thickness below the bottom fifth percentile of the normative database, glaucomatous ONH changes, and visual field defects on 24-2 tests.

Methods, Intervention, or Testing: POAG and control eyes were imaged using the OcuMet Beacon. A 23°x23° infrared scan was obtained, and an FPF scan was performed within a capture field spanning 13 degrees in diameter. The ONH margins on the infrared image were identified by software algorithms. FPF then was measured within an elliptical annulus around the ONH rim, with the inner and outer boundaries corresponding to 0.5 to 1.1 times the ONH rim size.

Main Outcomes Measures**:** FPF at the OHN rim in POAG and control eyes.

Results**:** Differences in FPF between POAG and control eyes were characterized through mixed-effects logistic regression, adjusted for age and interocular pressure. FPF was significantly higher in POAG versus control eyes, with a mean±SD of 46.4±27.9 versus 28.0±11.7 (P<0.001), respectively. Evaluation of anatomical quadrants revealed greater FPF in POAG versus control eyes at the temporal (P=0.001), superior (P<0.001), nasal (P=0.002), and inferior (P=0.001) quadrants. Among POAG eyes, FPF showed correlation to visual field mean deviation (P<0.001), visual field pattern standard deviation (P=0.003), and circumpapillary retinal nerve fiber thickness (P=0.001) on linear mixed-effects models.

Conclusions**:** Higher FPF in POAG versus control eyes suggests the presence of mitochondrial dysfunction at the ONH rim in eyes with glaucomatous damage. The degree of FPF corresponds to disease severity,

as measured by visual field and nerve fiber layer thickness metrics. FPF may thus represent a metabolic indicator of disease status that reveals the extent of injury in glaucoma.

Introduction

Glaucoma is a group of optic neuropathies characterized by the progressive degeneration and loss of retinal ganglion cells (RGC). It remains a major cause of blindness, globally impacting an estimated population of 80 million.[1] Early diagnosis is a key preventative measure against progression and blindness because patients may remain visually asymptomatic until late in the disease process and after irreversible damage.[2, 3] In addition, starting therapy during early stages of disease is shown to improve treatment efficacy and long-term outcomes.[4, 5] Current diagnosis is based on a constellation of imaging and clinical characteristics. This includes both structural changes involving the optic nerve head (ONH) and functional vision loss on perimetry.[6] Among clinical factors, elevated intraocular pressure (IOP) is the most important known risk factor for glaucoma development and progression. It has been utilized for screening, progression, and treatment and remains the only modifiable factor for slowing disease progression.[7, 8] Much, however, continues to be uncertain about the underlying causes of glaucoma, particularly for subtypes not fully explained by elevated IOP, such as normal-tension glaucoma (NTG). This has led to exploration of additional disease mechanisms, with attempts to elucidate accompanying novel biomarkers.

Recent studies have proposed mitochondrial dysfunction and death as a mechanism of glaucomatous damage.[9-11] Mitochondria serve multiple intracellular functions – including aerobic energy production, synaptic transmission, and mediation of apoptosis. These organelles reside densely in tissues with high metabolic requirements, including the laminar and prelaminar optic nerve.[12] Mitochondrial distribution in this region is shown to correspond with histological markers of metabolic activity and locations of concentrated ion channels involved in signal conduction.[13, 14] Dysregulation of mitochondrial proteins has, in turn, been linked to cellular stress and accumulation of reactive oxygen species (ROS).[15, 16] These events have been shown to trigger RGC injury and loss by apoptosis,[17-19] a mode of cell death implicated in glaucoma.[20, 21] Mitochondrial mutations, which may increase

susceptibility to dysfunction, have been documented for optic neuropathies, including primary open-angle glaucoma.[22] Alterations of mitochondria at the optic nerve have furthermore been identified through ex vivo imaging in mice models of glaucoma.[23, 24]

In human subjects, mitochondrial dysfunction has been characterized by measuring the presence of oxidized mitochondrial flavoproteins, which increase under conditions of cellular stress and increased ROS. Oxidized flavoproteins can be quantified by their emission of green fluorescence, termed flavoprotein fluorescence (FPF), upon stimulation by wavelengths of blue light.[25, 26] Elevated levels of FPF have been documented in a variety of ocular pathologies, including diabetic retinopathy[27], pseudotumor cerebri[28], central serous retinopathy[29], and age-related macular degeneration[30]. Increased FPF has also been seen in patients with primary open angle glaucoma and ocular hypertension within the macula.[31] As a precursor to cell death and tissue damage, FPF may thus provide an early indication of retinal dysfunction prior to structural changes or vision loss. In this study, we investigated FPF at the ONH as a potential biomarker for sub-structural glaucomatous injury in primary open-angle glaucoma.

Methods

Study Population

This retrospective study was performed in the Einhorn Clinical Research Center of the New York Eye and Ear Infirmary of Mount Sinai. The protocol was approved by the Institutional Review Board of Mount Sinai and is in accordance to the Declaration of Helsinki. All subjects were enrolled from November 2015 to October 2016 through written informed consent. On the day of imaging, medical history was obtained by interview and intraocular pressure was measured by Tono-Pen tonometry (Reichert Technologies, Depew, NY). Goldmann applanation tonometry was avoided since application of topical fluorescein would confound the FPF signal. Within one month of FPF imaging, all subjects received a comprehensive eye exam, which included slit-lamp biomicroscopy, gonioscopy, and fundoscopy.

Inclusion criteria for POAG eyes were natural lens, patient age >40 years, best-corrected visual acuity >20/200, open-angles on gonioscopy (Shaffer grade 3 or 4), and presence of POAG. POAG was defined by the presence of circumpapillary retinal nerve fiber layer thickness (cpRNFLT) below the bottom fifth percentile of the normative database as measured by optical coherence tomography (Spectralis, Heidelberg Engineering, Heidelberg, Germany), glaucomatous ONH changes (presence of rim thinning or notching), and visual field defects on 24-2 visual field testing (Humphrey Field Analyzer II, Carl Zeiss Meditec, Inc., Jena, Germany). Visual field defects were defined as three contiguous points at a 5% level on the pattern deviation plot with one of the three points at a 1% level, a glaucoma hemifield test outside normal limits, or a pattern standard deviation to a significance of <0.5%. Sufficient exam reliability was defined as having fewer than 20% fixation losses, 20% false negatives, and 20% false positives.

Inclusion criteria for control eyes were natural lens, patient age >40 years, best-corrected visual acuity better than 20/200, IOP <21mmHg, cpRNFLT above the bottom fifth percentile of the normative database on optical coherence tomography imaging, no visual field defects as defined above, and no evidence of optic nerve or retinal pathology on examination.

Exclusion criteria for all subjects were significant cataract (nuclear sclerosis grade >3, cortical, or posterior subcapsular cataract), pathology or surgery impacting the corneal curvature, intraocular surgery within 6 months prior to imaging, retinal disease, non-glaucomatous optic nerve pathology, diabetes mellitus, systemic inflammatory conditions, systemic immunodeficiency syndromes (including the human immunodeficiency virus), corticosteroid use, systemic immunosuppression, or neurodegenerative disorders (including Alzheimer's disease and Parkinson's disease).

Ancillary Tests

Optical coherence tomography (Spectralis, Heidelberg Engineering, Heidelberg, Germany) was used to measure cpRNFLT after dilation with one drop in each eye of phenylephrine hydrochloride ophthalmic

solution USP 2.5% (Paragon BioTeck, Inc., Portland, OR) and tropicamide hydrochloride ophthalmic solution USP 1% (Sandoz, Inc., Princeton, NJ). The global cpRNFLT was derived from the standard 3.45 mm-diameter circle scan centered at the ONH. Optical coherence tomography images were reviewed to confirm sufficient quality (signal strength >20) and to ensure correct segmentation of retinal layers.

Visual field tests were obtained for patients using the 24-2 SITA-standard test protocol (Humphrey Field Analyzer II Carl Zeiss Meditec, Inc., Jena, Germany) with the size III white stimulus.

Metabolic Image Acquisition and Processing

FPF at the ONH was measured using the OcuMet Beacon (OcuSciences, Ann Arbor, MI; Investigational Device). Light safety for the OcuMet Beacon has been evaluated and found to meet the International Electrotechnical Commission's guidelines, with the device classified under the safest laser/light emitting diode category: Type I. During each acquisition, the instrument captured a 23°x23° infrared fundus image and measured the FPF within a central 13°-diameter circular capture field (**Figure 1A**). The 512x512 detector generated FPF images with intensity measured as a dimensionless gray scale unit (gsu). Algorithmic evaluation of image quality selected the highest-contrast (indicating good illumination with minimal interference from pupil cropping) of several images captured at each session.

Software algorithms identified the ONH margins on the infrared image and demarcated an elliptical annulus around the ONH rim, with inner and outer boundaries corresponding to 0.5 to 1.1 times the ONH rim size (**Figure 1B**). The region bound by this annulus captures the highest concentration of FPF signal, which is consistent with the distribution of mitochondria at the ONH. The mean FPF score of the tissue outside the ONH (typically 25-30 gsu) was then subtracted from the measured disc profile, as this was found to improve the OD-OS match in healthy controls. The annulus was then divided into fifty sectors, with global FPF defined as the average of all sectors. Averages of sectors for each anatomical region (temporal, superior, nasal, and inferior) were also determined. An FPF sector map was created, which displayed FPF levels circumferentially across the anatomical quadrants (**Figure 1C**).

Averaged FPF throughout the ONH annulus and at each anatomical location were then summarized through an FPF profile that permits rapid comparison to the average of healthy controls (**Figure 1D**).

Statistical Analysis

Analyses were performed using SPSS 27 software (IBM Corporation, Chicago, IL, USA). Clinical metrics were evaluated for normality. Comparisons of clinical metrics (including IOP, cpRNFLT, and number of ocular antihypertensive medications) between POAG and control eyes were performed using mixed-effects models to account for interocular correlations. Differences in FPF between POAG and control subjects were then analyzed through mixed-effects logistic regressions, with the disease state as the dependent variable and FPF as the independent variable.

Correlations between FPF and clinical characteristics of IOP and age were evaluated using linear mixed-effects models, with the FPF as the dependent variable and the clinical features as the independent variable. The relationship between FPF and existing glaucoma metrics was also examined while accounting for IOP and age. These metrics included visual field mean deviation, visual field pattern standard deviation, and cpRNFLT.

Intra-visit repeatability of OcuMet Beacon scans at the ONH was characterized using the coefficient of variation. This metric was based on four sequential images from a representative POAG patient eye and from a control subject eye, with calculations derived from the standard deviation of obtained FPF values divided by the mean of the FPF measurements.

Results

Patient Characteristics

Results were obtained from 50 eyes of 30 POAG patients and 36 eyes of 20 healthy controls. Participant characteristics are shown in **Table 1**. Comparison of clinical metrics between POAG and control eyes demonstrated significant differences in the number of antihypertensive

medications, IOP, and global cpRNFLT. POAG and control subjects were respectively comprised of 51.4% and 53.2% male participants. No statistically significant difference in age was found between the two groups.

Intra-visit Repeatability

The coefficients of variation for FPF in POAG and control eyes were 8.2% and 10.5%, respectively.

Comparison of FPF between POAG and Control Eyes

Circumferential representations of FPF for the mean of POAG and control eyes are shown in **Figure 2**. Both POAG and control subjects revealed a similar pattern of FPF fluctuation across anatomical quadrants, with higher mean FPF was exhibited by POAG eyes throughout the ONH compared to healthy controls. Multivariate analysis accounting for patient age and IOP demonstrated a statistically significant difference in global FPF between POAG and control eyes (46.4±27.9 vs. 28.0±11.7, respectively) (**Table 2**). Significant differences were also found at all anatomical quadrants. Representative POAG and control eyes are shown in **Figure 3**.

Correlation of FPF to Clinical Characteristics

Among POAG eyes, global FPF exhibited a positive correlation with patient age and no correlation with IOP (**Table 3**). POAG eyes also demonstrated relationships between global FPF and clinical biomarkers of glaucoma: a negative correlation with visual field mean deviation, a positive correlation with visual field pattern standard deviation, and a negative correlation with global cpRNFLT. Significant correlations were also present between sectoral FPF and the corresponding cpRNFLT at the superior, inferior, and nasal quadrants.

Discussion

This cross-sectional study is, to our knowledge, the first investigation of in vivo mitochondrial dysfunction in POAG eyes at the ONH. Statistical analyses revealed significantly higher FPF in POAG eyes

compared to controls, with differences observed at all anatomical quadrants. These findings suggest the presence of increased mitochondrial dysfunction throughout the ONH and the potential for FPF to serve as an additional means to evaluate glaucomatous damage. These measurements may have particular utility for identifying disease status in patients without elevated IOP. Evaluation of FPF may also facilitate investigation of neuroprotective therapies for glaucoma. Animal studies have identified agents that offer potential protection against cellular stress and RGC apoptosis.[32-35] Efficacy of these agents, however, has generally not translated to human subjects, with challenges attributed to current in vivo metrics and possibly narrow therapeutic windows. Characterization of metabolic changes in RGC may provide a more sensitive means of evaluating treatment effect. In addition, recent studies have identified stages of RGC injury that precede irreversible RGC in glaucoma.[36-39] These pre-apoptotic changes to RGC may be reflected in mitochondrial dysfunction and serve as a method for evaluating neuroprotective agents.

FPF also exhibited statistically significant correlations with existing imaging markers of disease severity. FPF exhibited a negative correlation with visual field mean deviation and a positive correlation with visual field pattern standard deviation, suggesting that the severity of mitochondrial dysfunction in glaucoma may be related to the extent of vision loss. A negative correlation was also seen in POAG eyes between FPF and cpRNFLT of the entire imaging annulus, suggesting that increased mitochondrial dysfunction is present with greater structural glaucomatous changes at the ONH. Comparison of FPF to clinical characteristics in POAG eyes revealed a positive correlation between FPF and age, supporting previous studies. No correlation was present between FPF and IOP among POAG eyes. This may be influenced by the use of ocular antihypertensive therapy by patients, some of which have been documented to exert neuroprotective effects independent of their alternation of aqueous humor production or reabsorption.[40, 41] Previous studies reporting positive correlations between IOP and

mitochondrial dysfunction used cellular and animal models of glaucoma not confounded by ongoing medical therapy.[24, 42]

Limitations of the study include enrollment of patients after initiation of medical therapy. Compared to a study of treatment naïve patients, inclusion of previous-treated patients may artificially decrease the difference in FPF between POAG and control subjects due to the impact of therapy on mitochondrial dysfunction and FPF. While no studies have evaluated the impact of ocular antihypertensives on FPF, past rodent studies have suggested independent neuroprotective effects of IOP lowering agents, which are hypothesized to involve mitochondria-mediated apoptosis of RGC.[40, 41] Comparison of FPF to visual field measurements as a metric of functional change may also be impacted by previously documented variability of visual field results, particularly among patients with severe disease. In addition, the cross-sectional nature of this study limits the ability to demonstrate casualty of glaucomatous change due to mitochondrial dysfunction at the ONH.

Future areas of research include a comparison of FPF between healthy controls and glaucoma suspects or patients with mild glaucomatous changes. Given that changes in mitochondrial movement were seen prior to axonal structural alterations after IOP elevation in rodent models, we surmise that changes in FPF would be observed prior to structural glaucomatous damage in human subjects.[24] This may provide an additional objective means to evaluate and differentiate early stages of glaucoma from healthy controls. Longitudinal studies focusing on impact of ocular antihypertensives may also provide meaningful information the neuroprotective role of existing medications.

Overall, greater FPF at the ONH rim was found in POAG eyes compared to control eyes, which is consistent with previous studies showing increased mitochondrial dysfunction in eyes with glaucomatous damage. Among POAG eyes, correlations were also found between FPF and existing metrics of glaucoma severity. These results highlight the potential of FPF in characterizing glaucoma status and exploring disease pathophysiology. Future longitudinal investigations of FPF may clarify its

role for assessing disease progression and characterizing the efficacy of neuroprotective therapies. Evaluation of FPF in other glaucoma subtypes may also provide insight into mechanisms of disease for individuals without elevations in intraocular pressure.

Figure 1: Methodology of FPF Analysis at the Optic Nerve Head

A) 23°x23° infrared image of a representative POAG eye. The green circle highlights the central circular FPF capture field spanning 13 degrees in diameter. The white ellipse indicates the algorithmically identified optic nerve head (ONH).

B) Green and white rings correspond to same features as in (A). Subtraction of background lens fluorescence was performed based on readings sampled outside the blue circle. Measurement at the ONH is taken between inner and outer red ellipses generated respectively at ratiometric distances 0.5 and 1.1 times the white ONH ellipse perimeter. This annulus captures the highest concentration of FPF signal, which is consistent with the distribution of mitochondria at the ONH, with the central area occupied by retinal vasculature. The mean FPF score of the tissue outside the ONH (typically 25-30 gsu) was then subtracted from the measured disc profile, as this was found to improve the OD-OS match in healthy controls.

C) FPF sector map. Measured FPF from each of the 50 sectors is indicated by the black line. For comparison, the green line and surrounding green area represent the mean ± one standard deviation of FPF in healthy controls. Figure axis and orientation follow a circumferential format, with TMP=temporal, SUP=superior, NAS=nasal, INF=inferior.

D) FPF profile of the same eye. Averaged measurements from each anatomical sector are displayed in the black text. Reference mean FPF from healthy controls are presented in the green text. The center region represents the global average of all FPF sectors. N=nasal, I=inferior, T=temporal, and S=superior.

Figure 2: Visualization of Mean FPF Between Groups

Representation of the mean FPF of POAG and control eyes across anatomical sectors, using a circumferential axis format. TMP=temporal, SUP=superior, NAS=nasal, and INF=inferior. Higher levels of FPF are seen in POAG eyes compared to healthy controls, with greater FPF across all anatomic sectors.

Figure 3: FPF Measurements from Representative POAG and Control Eyes

FPF analysis for representative control and POAG eyes showing the A) infrared image B) FPF heatmap C) FPF sector maps, and D) FPF profile. Greater scores can be observed in the POAG eye compared to the healthy control on both the FPF sector map and profile.

References

1. Quigley HA, Broman AT. The number of people with glaucoma worldwide in 2010 and 2020. *Br J Ophthalmol*. Mar 2006;90(3):262-7. doi:10.1136/bjo.2005.081224
2. Rotchford AP, Kirwan JF, Muller MA, Johnson GJ, Roux P. Temba glaucoma study: a population-based cross-sectional survey in urban South Africa. *Ophthalmology*. Feb 2003;110(2):376-82. doi:10.1016/s0161-6420(02)01568-3
3. Sommer A, Tielsch JM, Katz J, et al. Relationship between intraocular pressure and primary open angle glaucoma among white and black Americans. The Baltimore Eye Survey. *Arch Ophthalmol*. Aug 1991;109(8):1090-5. doi:10.1001/archopht.1991.01080080050026
4. De Moraes CG, Demirel S, Gardiner SK, et al. Effect of treatment on the rate of visual field change in the ocular hypertension treatment study observation group. *Invest Ophthalmol Vis Sci*. Apr 2 2012;53(4):1704-9. doi:10.1167/iovs.11-8186
5. Hattenhauer MG, Johnson DH, Ing HH, et al. The probability of blindness from open-angle glaucoma. *Ophthalmology*. Nov 1998;105(11):2099-104. doi:10.1016/s0161-6420(98)91133-2
6. Susanna R, Jr., De Moraes CG, Cioffi GA, Ritch R. Why do people (still) go blind from glaucoma? *Transl Vis Sci Technol*. Mar 2015;4(2):1. doi:10.1167/tvst.4.2.1
7. Musch DC, Gillespie BW, Niziol LM, Lichter PR, Varma R. Intraocular pressure control and long-term visual field loss in the Collaborative Initial Glaucoma Treatment Study. *Ophthalmology*. 2011/09/01/ 2011;118(9):1766-1773. doi:https://doi.org/10.1016/j.ophtha.2011.01.047
8. Sommer A. Intraocular pressure and glaucoma. *Am J Ophthalmol*. 1989;107(2):186-188.
9. Korsmeyer SJ, Shutter JR, Veis DJ, Merry DE, Oltvai ZN. Bcl-2/Bax: a rheostat that regulates an anti-oxidant pathway and cell death. *Semin Cancer Biol*. Dec 1993;4(6):327-32.
10. Elner SG, Elner VM, Field MG, Park S, Heckenlively JR, Petty HR. Retinal flavoprotein autofluorescence as a measure of retinal health. *Trans Am Ophthalmol Soc*. 2008;106:215-22; discussion 222-4.
11. Williams PA, Harder JM, Foxworth NE, et al. Vitamin B3 modulates mitochondrial vulnerability and prevents glaucoma in aged mice. *Science*. 2017;355(6326):756-760.
12. Wang L, Dong J, Cull G, Fortune B, Cioffi GA. Varicosities of intraretinal ganglion cell axons in human and nonhuman primates. *Invest Ophthalmol Vis Sci*. 2003;44(1):2-9. doi:10.1167/iovs.02-0333
13. Barron MJ, Griffiths P, Turnbull DM, Bates D, Nichols P. The distributions of mitochondria and sodium channels reflect the specific energy requirements and conduction properties of the human optic nerve head. *Br J Ophthalmol*. Feb 2004;88(2):286-90. doi:10.1136/bjo.2003.027664

14. Bristow EA, Griffiths PG, Andrews RM, Johnson MA, Turnbull DM. The distribution of mitochondrial activity in relation to optic nerve structure. *Arch Ophthalmol*. Jun 2002;120(6):791-6. doi:10.1001/archopht.120.6.791
15. Kroemer G, Reed JC. Mitochondrial control of cell death. *Nat Med*. May 2000;6(5):513-9. doi:10.1038/74994
16. Maresca A, la Morgia C, Caporali L, Valentino ML, Carelli V. The optic nerve: a "mito-window" on mitochondrial neurodegeneration. *Mol Cell Neurosci*. Jul 2013;55(100):62-76. doi:10.1016/j.mcn.2012.08.004
17. Levin LA, Clark JA, Johns LK. Effect of lipid peroxidation inhibition on retinal ganglion cell death. *Invest Ophthalmol Vis Sci*. Dec 1996;37(13):2744-9.
18. Lieven CJ, Vrabec JP, Levin LA. The effects of oxidative stress on mitochondrial transmembrane potential in retinal ganglion cells. *Antioxid Redox Signal*. 2003/10/01 2003;5(5):641-646. doi:10.1089/152308603770310310
19. Charles I, Khalyfa A, Kumar DM, et al. Serum deprivation induces apoptotic cell death of transformed rat retinal ganglion cells via mitochondrial signaling pathways. *Invest Ophthalmol Vis Sci*. 2005;46(4):1330-1338. doi:10.1167/iovs.04-0363
20. Quigley HA, Nickells RW, Kerrigan LA, Pease ME, Thibault DJ, Zack DJ. Retinal ganglion cell death in experimental glaucoma and after axotomy occurs by apoptosis. *Invest Ophthalmol Vis Sci*. 1995;36(5):774-786.
21. Garcia-Valenzuela E, Shareef S, Walsh J, Sharma SC. Programmed cell death of retinal ganglion cells during experimental glaucoma. *Exp Eye Res*. 1995/07/01/ 1995;61(1):33-44. doi:https://doi.org/10.1016/S0014-4835(95)80056-5
22. Abu-Amero KK, Morales J, Bosley TM. Mitochondrial abnormalities in patients with primary open-angle glaucoma. *Invest Ophthalmol Vis Sci*. 2006;47(6):2533-2541. doi:10.1167/iovs.05-1639
23. Zhu Y, Pappas AC, Wang R, Seifert P, Sun D, Jakobs TC. Ultrastructural morphology of the optic nerve head in aged and glaucomatous mice. *Invest Ophthalmol Vis Sci*. Aug 1 2018;59(10):3984-3996. doi:10.1167/iovs.18-23885
24. Kimball EC, Pease ME, Steinhart MR, et al. A mouse ocular explant model that enables the study of living optic nerve head events after acute and chronic intraocular pressure elevation: Focusing on retinal ganglion cell axons and mitochondria. *Exp Eye Res*. 2017/07/01/ 2017;160:106-115. doi:https://doi.org/10.1016/j.exer.2017.04.003
25. Benson RC, Meyer RA, Zaruba ME, McKhann GM. Cellular autofluorescence--is it due to flavins? *J Histochem Cytochem*. Jan 1979;27(1):44-8. doi:10.1177/27.1.438504
26. Reinert KC, Dunbar RL, Gao W, Chen G, Ebner TJ. Flavoprotein autofluorescence imaging of neuronal activation in the cerebellar cortex in vivo. *J Neurophysiol*. Jul 2004;92(1):199-211. doi:10.1152/jn.01275.2003
27. Field MG, Elner VM, Puro DG, et al. Rapid, noninvasive detection of diabetes-induced retinal metabolic stress. *Arch Ophthalmol*. Jul 2008;126(7):934-8. doi:10.1001/archopht.126.7.934
28. Elner VM, Park S, Cornblath W, Hackel R, Petty HR. Flavoprotein autofluorescence detection of early ocular dysfunction. *Arch Ophthalmol*. Feb 2008;126(2):259-60. doi:10.1001/archophthalmol.2007.44
29. Field MG, Elner VM, Park S, et al. Detection of retinal metabolic stress resulting from central serous retinopathy. *Retina*. Sep 2009;29(8):1162-6. doi:10.1097/IAE.0b013e3181a3b923
30. Field MG, Comer GM, Kawaji T, Petty HR, Elner VM. Noninvasive imaging of mitochondrial dysfunction in dry age-related macular degeneration. *Ophthalmic Surg Lasers Imaging*. Sep-Oct 2012;43(5):358-65. doi:10.3928/15428877-20120712-02

31. Geyman LS, Suwan Y, Garg R, et al. Noninvasive detection of mitochondrial dysfunction in ocular hypertension and primary open-angle glaucoma. *J Glaucoma*. 2018;27(7):592-599. doi:10.1097/ijg.0000000000000980
32. Saylor M, McLoon LK, Harrison AR, Lee MS. Experimental and clinical evidence for brimonidine as an optic nerve and retinal neuroprotective agent: an evidence-based review. *Arch Ophthalmol*. Apr 2009;127(4):402-6. doi:10.1001/archophthalmol.2009.9
33. Abdel-Kader R, Hauptmann S, Keil U, et al. Stabilization of mitochondrial function by Ginkgo biloba extract (EGb 761). *Pharmacol Res*. 2007/12/01/ 2007;56(6):493-502. doi:https://doi.org/10.1016/j.phrs.2007.09.011
34. Jiang W, Tang L, Zeng J, Chen B. Adeno-associated virus mediated SOD gene therapy protects the retinal ganglion cells from chronic intraocular pressure elevation induced injury via attenuating oxidative stress and improving mitochondrial dysfunction in a rat model. *Am J Transl Res*. 2016;8(2):799-810.
35. Lee D, Shim MS, Kim K-Y, et al. Coenzyme Q10 inhibits glutamate excitotoxicity and oxidative stress–mediated mitochondrial alteration in a mouse model of glaucoma. *Invest Ophthalmol Vis Sci*. 2014;55(2):993-1005. doi:10.1167/iovs.13-12564
36. Jeon SJ, Park HL, Jung KI, Park CK. Relationship between pattern electroretinogram and optic disc morphology in glaucoma. *PLoS One*. 2019;14(11):e0220992. doi:10.1371/journal.pone.0220992
37. Kerrigan-Baumrind LA, Quigley HA, Pease ME, Kerrigan DF, Mitchell RS. Number of ganglion cells in glaucoma eyes compared with threshold visual field tests in the same persons. *Invest Ophthalmol Vis Sci*. Mar 2000;41(3):741-8.
38. Porciatti V, Nagaraju M. Head-up tilt lowers IOP and improves RGC dysfunction in glaucomatous DBA/2J mice. *Exp Eye Res*. 2010/03/01/ 2010;90(3):452-460. doi:https://doi.org/10.1016/j.exer.2009.12.005
39. Sehi M, Grewal DS, Goodkin ML, Greenfield DS. Reversal of retinal ganglion cell dysfunction after surgical reduction of intraocular pressure. *Ophthalmology*. 2010/12/01/ 2010;117(12):2329-2336. doi:https://doi.org/10.1016/j.ophtha.2010.08.049
40. Wheeler L, WoldeMussie E, Lai R. Role of alpha-2 agonists in neuroprotection. *Surv Ophthalmol*. 2003/04/01/ 2003;48(2, Supplement):S47-S51. doi:https://doi.org/10.1016/S0039-6257(03)00004-3
41. Hernández M, Urcola JH, Vecino E. Retinal ganglion cell neuroprotection in a rat model of glaucoma following brimonidine, latanoprost or combined treatments. *Exp Eye Res*. 2008/05/01/ 2008;86(5):798-806. doi:https://doi.org/10.1016/j.exer.2008.02.008
42. Ju W-K, Liu Q, Kim K-Y, et al. Elevated hydrostatic pressure triggers mitochondrial fission and decreases cellular ATP in differentiated RGC-5 cells. *Invest Ophthalmol Vis Sci*. 2007;48(5):2145-2151. doi:10.1167/iovs.06-0573

Table 1: Participant Characteristics

Clinical Characteristic	POAG† (n = 50)	Control† (n = 36)	POAG versus Control Comparison			
			Coefficient	95% CI Lower	95 % CI Upper	P-Value
Age (years)	57.0 ± 8.2	55 ± 9	-1.98	-5.72	1.75	0.294
Number of Ocular Antihypertensive Medications	4.1 ± 3.0	0 ± 0	-2.70	-3.14	-2.25	< 0.001
IOP (mmHg)	18.7 ± 5.6	15.9 ± 3.3	-2.82	-4.83	-0.81	0.007
cpRNFLT (µm)	72.9 ± 22.9	101.9 ± 8.2	28.95	21.35	36.56	< 0.001

†Values are reported as mean ± standard deviation

POAG = primary open angle glaucoma; IOP = intraocular pressure; cpRNFLT = circumpapillary retinal nerve fiber layer thickness; CI = confidence interval

Table 2: Difference in FPF Between POAG and Control Eyes

FPF Region	POAG† (n = 50)	Control† (n = 36)	POAG versus Control Comparison			
			Coefficient	95 % CI Lower	95 % CI Upper	P-Value
Global	46.4 ± 27.9	28.0 ± 11.7	0.085	0.040	0.129	< 0.001
Temporal	68.5 ± 40.3	49.1 ± 21.1	0.034	0.014	0.054	0.001
Superior	32.8 ± 29.5	10.3 ± 9.3	0.120	0.070	0.170	< 0.001
Nasal	39.7 ± 27.1	25.1 ± 15.3	0.045	0.017	0.074	0.002
Inferior	45.9 ± 28.9	29.0 ± 11.1	0.049	0.021	0.078	0.001

†Values are reported as mean ± standard deviation

FPF = flavoprotein fluorescence; POAG = primary open angle glaucoma; CI = confidence interval

Table 3: Correlations between FPF and Clinical Characteristics

Clinical Characteristic	Coefficient	95 % CI Lower*	95 % CI Upper*	P-Value
Age	1.361	0.251	2.471	0.02
IOP	-0.780	-1.812	0.252	0.14

IOP = intraocular pressure; CI = confidence interval.

Table 4. Comparison of FPF and Metrics of Disease Severity

Clinical Characteristic	Coefficient	95 % CI Lower*	95 % CI Upper*	P-Value
VF MD	-0.996	-1.445	-0.548	< 0.001
VF PSD	2.860	1.010	4.710	0.003
cpRNFLT Global	-0.388	-0.616	-0.161	0.001
cpRNFLT Temporal	0.185	-0.549	0.920	0.611
cpRNFLT Superior	-0.203	-0.390	-0.015	0.035
cpRNFLT Nasal	-0.341	-0.613	-0.069	0.015
cpRNFLT Inferior	-0.283	-0.478	-0.088	0.006

FPF = flavoprotein fluorescence; VF MD = visual field mean deviation; VF PSD = visual field pattern standard deviation; cpRNFLT = circumpapillary retinal nerve fiber layer thickness; CI = confidence interval. Linear mixed model analysis accounted for IOP and age of patients.

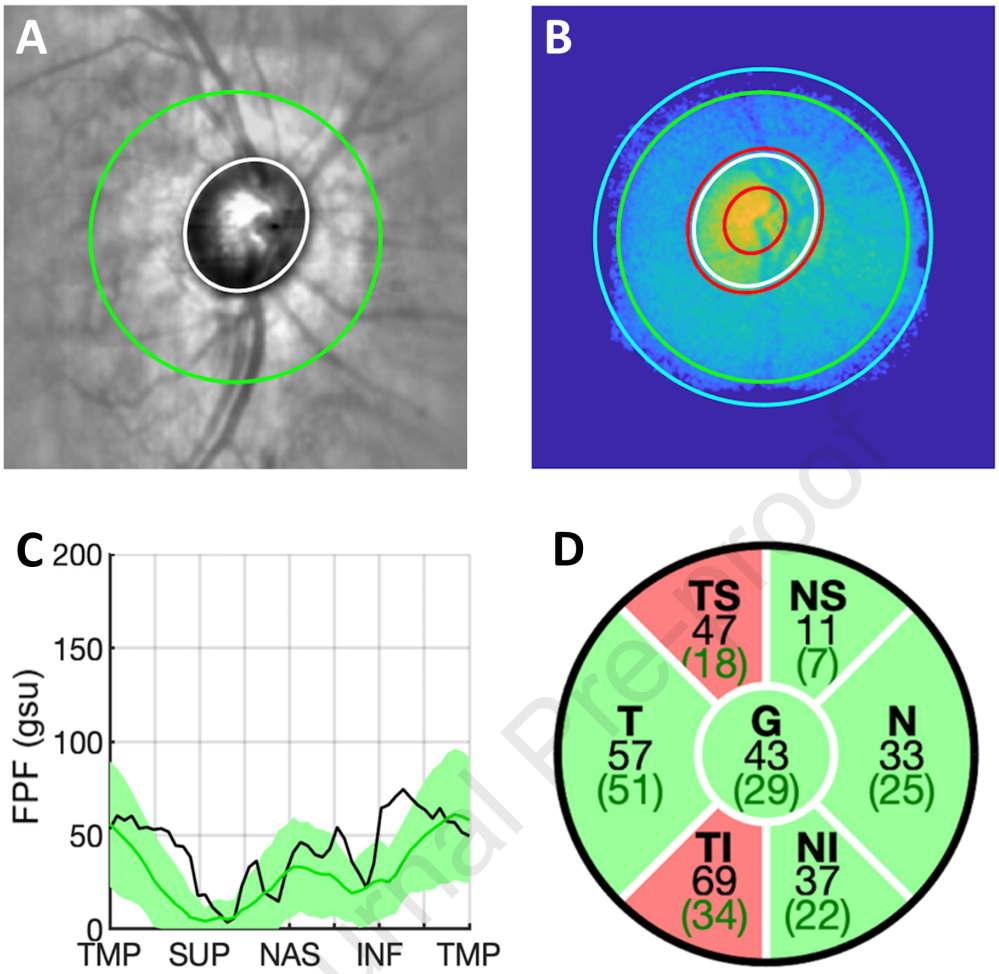

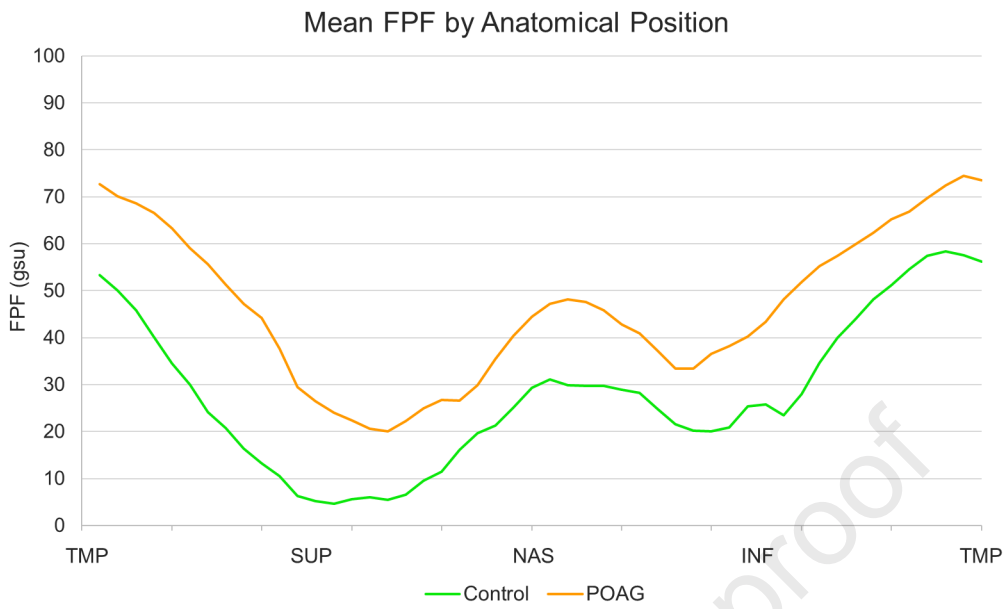

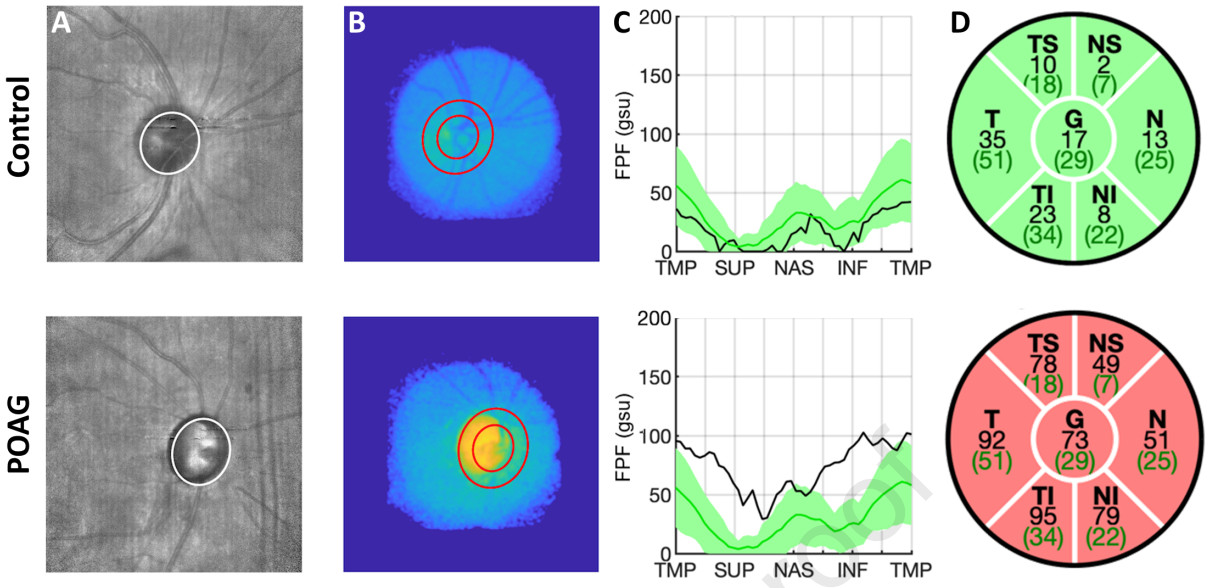

Précis: Flavoprotein fluorescence at the optic nerve head reveals mitochondrial dysfunction in primary open-angle glaucoma eyes compared to healthy controls, with correlations to existing metrics of glaucomatous damage.